

Lecture 23: Liquid Motors: Stability (High Frequency); Acoustics

Combustion Instability: High Frequency

Methods of Analysis for High Frequency Instabilities

Prior to the advent of large-scale computations, the most successful theoretical development in this area was the “sensitive time lag theory” of L. Crocco [26]. More than a detailed physical theory, this was a model in which a few basic parameters were introduced from intuitive considerations, and then used to correlate experimental observations on stability thresholds. The principal parameter was the sensitive time lag, during which the various rates which eventually resulted in vaporization at the total time lag τ_T after injection were assumed to vary with pressure, velocity, stoichiometry, etc. This variation was characterized by means of other important parameter, the “sensitivity index”. For pressure sensitivity, this is

$$n = \frac{\partial \ln(\text{Rates})}{\partial \ln P} \quad (1)$$

and the definition of τ is such that the variations in gas generation rate due to this sensitivity are given locally by

$$\frac{\dot{\bar{m}} - \bar{\dot{m}}}{\bar{\dot{m}}} = -\frac{\partial \tau}{\partial t} = n \frac{P'(t) - P'(t - \tau)}{\bar{P}} \quad (2)$$

Similar sensitivity indices can be introduced for velocity, etc. Once this parameterization is accepted, it is only a matter of mathematical modeling to obtain the stability limits of a given acoustic wave or cavity. This modeling could be linear or even allow for non-linearities in the gas dynamics. It is one of the strengths of this theory that the acoustic part of the problem, namely, combustor geometry, steady state combustion and heat release, etc. are separated from the unsteady combustion effects, which allows for generalization of test results and accumulation of meaningful stability data.

The results of calculations using the linear sensitive time lag theory are displayed as shown in Fig. 1 (Ref. 26).

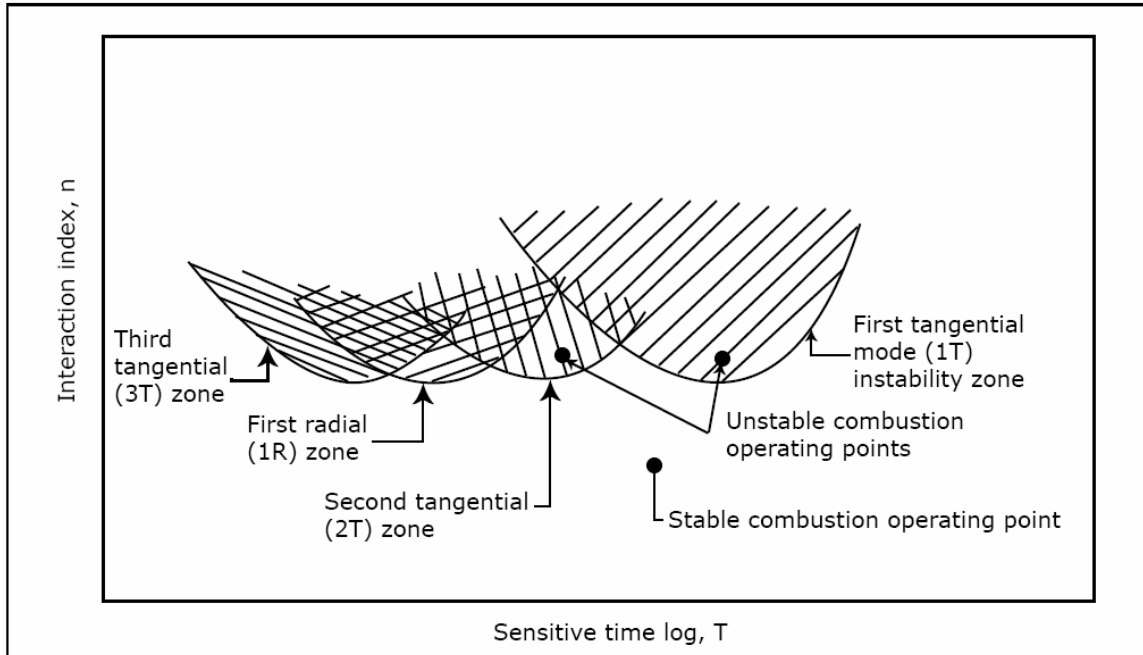
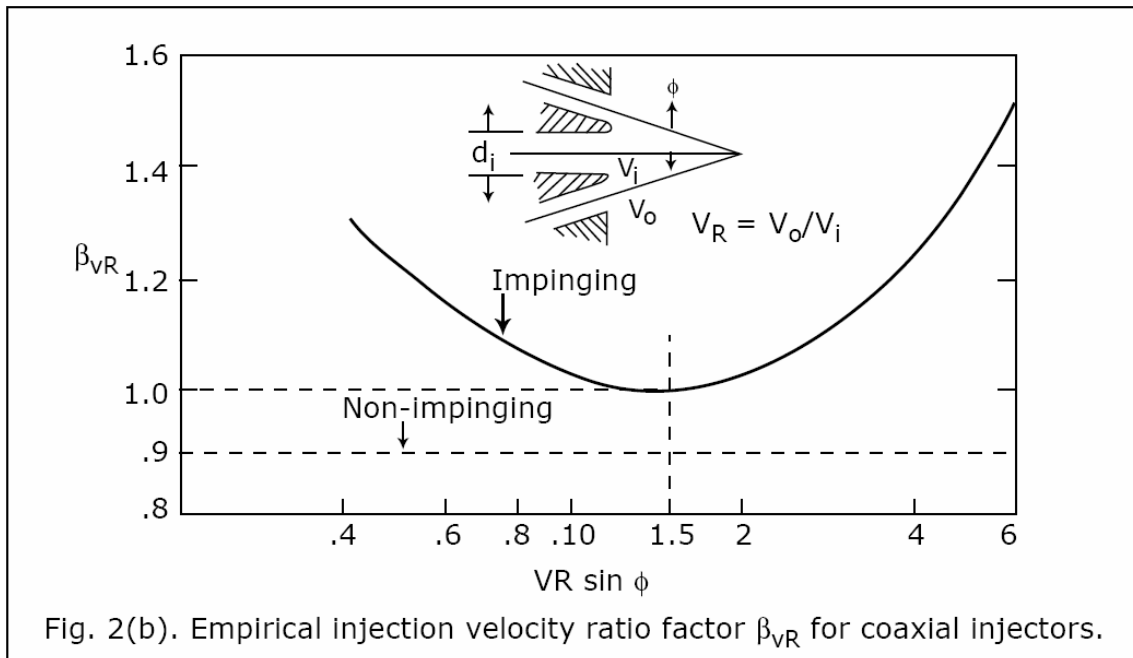
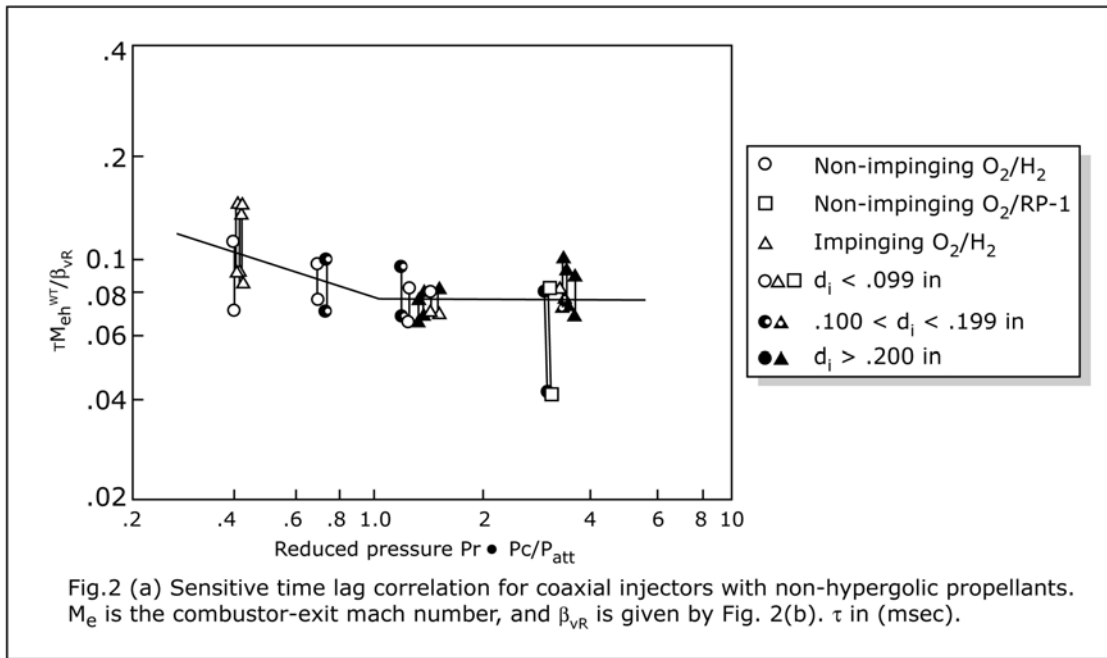


Fig 1. An $n-\tau$ diagram, showing instability zones for various modes.

Here are shown the loci of marginal stability for severe modes of a combustor, on a map of interaction index n vs. sensitive lag τ . Each point on one of the lines corresponds to a particular oscillation frequency, and these frequencies are found to be within $\pm 10\%$ of the undisturbed acoustic frequency of the mode. The goal of the designer is to manipulate the factors influencing n and τ in order to place the operating point outside all the stable regions of the various modes.

The parameters τ and n (into which is lumped the modifying effects of velocity or other sensitivities) are basically empirical, and a large data base has been laboriously accumulated on their dependencies upon many design factors. As an example, Figs. 2(a) and 2(b) (Ref. 26) show data on τ for coaxial injectors, for which $n \cong 0.5$ throughout.



Starting with the early of Priem and Guentert [29], these methods have been progressively replaced by detailed numerical time-dependent simulations of the combustion process. The complexity of these processes is such that, even now these simulations still contain large elements of modeling and approximation, and are generally limited to one or two selected spatial dimension plus time.

A recent example of this approach is described in Ref. 30. Here the emphasis is on the tangential acoustic modes. A detailed 2-D fluid mechanical model (in the transverse plane) is coupled to a series of empirically derived droplet vaporization laws for UDMH and N_2O_4 . The flow is turbulent, modeled using a $K-\epsilon$ approximation, and the drops are allowed to slip, exerting drag forces which are computed from empirical drag coefficients, and also modifying the vaporization rates due to convective heat transfer. The drop-heating transients are ignored. The computations yield detailed time histories of all the fluid parameters, and comparisons to limited test data on parametric effects of pressure and injector type are found to be favorable.

A similar computation, but for longitudinal modes only, is described in Ref. 27. Here the spatial dependence is on one dimension only (axial), but the droplet interactions are calculated in somewhat more detail, including drop thermal inertia. These calculations show strongest instability when the ratio of the acoustic period to the droplet vaporization time is 0.15, which, as noted before, can be interpreted as indicating a "sensitive" time lag which is a fraction (0.1-0.2) of the total vaporization time. The calculations also show cases of entropy wave excitation, for which the frequency corresponds closely to the convective time in the chamber.

In what follows, we provide a simplified analysis of the acoustic effects of several combustion-related phenomena (heat release, mass addition, etc.), and then use this in conjunction with Crocco's theory for an assessment of stability in a simple 1-D situation. Some general conclusions about stability and destability effects are also drawn from the acoustic analysis.

Acoustic equations with heat and mass addition, fluid forces, and molecular mass changes.

$$\frac{\partial}{\partial z} = \frac{\partial}{\partial y} = 0$$

$$\begin{aligned}
 1. & \left\{ \begin{array}{l} \frac{\partial \rho}{\partial t} + \frac{\partial(\rho u)}{\partial x} = m \\ \rho \frac{\partial u}{\partial t} + \rho u \frac{\partial u}{\partial x} + \frac{\partial p}{\partial x} = f \\ c_v \left(\frac{\partial T}{\partial t} + u \frac{\partial T}{\partial x} \right) = \frac{q}{\rho} - p \left(\frac{\partial(1/\rho)}{\partial t} + u \frac{\partial(1/\rho)}{\partial x} \right) \\ \frac{p}{\rho} = \frac{R}{M} T \end{array} \right. \quad \begin{array}{l} \text{(mass addition p.u. volume, p.u. time)} \\ \text{(force p.u. volume)} \\ \text{(q=heating rate p.u. volume)} \end{array}
 \end{aligned}$$

Assume small perturbations about a uniform steady background, (with μ, m, f, q):

$$\rho = \bar{\rho} + \rho', \quad u = \bar{u} + u', \quad p = \bar{p} + p', \quad T = \bar{T} + T', \quad \mu = \bar{\mu} + \mu' \quad (5)$$

$$\begin{array}{c} \uparrow \\ \bar{u} = 0 \end{array} \quad (6)$$

Because of (6),

$$\frac{DQ}{Dt} \equiv \frac{\partial Q}{\partial t} + u \frac{\partial Q}{\partial x} = \frac{\partial Q'}{\partial t} + \left(\bar{\mu} + \mu' \right) \frac{\partial Q'}{\partial x} \approx \frac{\partial Q'}{\partial t} \quad (7)$$

$\begin{array}{c} \uparrow 0 \\ \bar{\mu} + \mu' \\ \downarrow \\ \text{2nd order} \end{array}$

Linearizing then,

$$\begin{array}{l}
 \frac{\partial \rho'}{\partial t} + \bar{\rho} \frac{\partial u'}{\partial x} = m \quad (8) \\
 \bar{\rho} \frac{\partial u'}{\partial t} + \frac{\partial p'}{\partial x} = f \quad (9) \\
 \bar{\rho} \bar{c}_v \frac{\partial T'}{\partial t} = q + \frac{\bar{p}}{\rho} \frac{\partial p'}{\partial t} \quad (10) \\
 \frac{p'}{\bar{p}} - \frac{\rho'}{\bar{\rho}} = \frac{T'}{\bar{T}} + \frac{M'}{M} \quad (11)
 \end{array}
 \left. \begin{array}{l} \\ \\ \\ \end{array} \right\} \begin{array}{l} \\ \rightarrow \\ \rightarrow \end{array} \begin{array}{l} \\ \bar{\rho} \frac{\partial^2 u'}{\partial x \partial t} + \frac{\partial^2 p'}{\partial x^2} = \frac{\partial f}{\partial x} \quad (12) \\ \\ T' = \bar{T} \left(\frac{p'}{\bar{p}} - \frac{\rho'}{\bar{\rho}} + \frac{\mu'}{\mu} \right) \quad (13) \end{array}$$

(13) into (10):

$$\bar{\rho} \bar{c}_v \bar{T} \left(\frac{1}{\bar{\rho}} \frac{\partial \bar{p}'}{\partial t} - \frac{1}{\bar{\rho}} \frac{\partial \bar{p}'}{\partial t} + \frac{1}{\bar{M}} \frac{\partial \bar{M}'}{\partial t} \right) = q + \frac{\bar{p}}{\bar{\rho}} \frac{\partial \bar{p}'}{\partial t}$$

$\frac{\bar{p}}{\bar{\rho}} = \frac{R}{M} \bar{T} = \bar{R}_g \bar{T}$

$$\bar{T} \underbrace{\left(\frac{R}{\bar{M}} + \bar{c}_v \right)}_{\bar{c}_p} \frac{\partial \bar{p}'}{\partial t} = -q + \frac{\bar{c}_v}{\bar{R}_g} \frac{\partial \bar{p}'}{\partial t} + \frac{\bar{p}}{\bar{\rho}} \frac{\bar{c}_v}{\bar{R}_g} \frac{\partial (\bar{M}'/\bar{M})}{\partial t}$$

$$\frac{\partial \bar{p}'}{\partial t} = \frac{1}{\bar{c}_p \bar{T}} \left[\frac{1}{\gamma - 1} \frac{\partial \bar{p}'}{\partial t} - q + \frac{\bar{p}}{\gamma - 1} \frac{\partial (\bar{M}'/\bar{M})}{\partial t} \right] \quad (14)$$

Sub. Into (8)

$$\frac{1}{\bar{c}_p \bar{T}} \left[\frac{1}{\gamma - 1} \frac{\partial \bar{p}'}{\partial t} - q + \frac{\bar{p}}{\gamma - 1} \frac{\partial (\bar{M}'/\bar{M})}{\partial t} \right] + \bar{\rho} \frac{\partial \bar{u}'}{\partial x} = m \quad (15)$$

Differentiate w.r.t. t:

$$\frac{1}{\bar{c}_p \bar{T}} \left[\frac{1}{\gamma - 1} \frac{\partial^2 \bar{p}'}{\partial t^2} - \frac{\partial q}{\partial t} + \frac{\bar{p}}{\gamma - 1} \frac{\partial^2 (\bar{M}'/\bar{M})}{\partial t^2} \right] + \bar{\rho} \frac{\partial^2 \bar{u}'}{\partial x \partial t} = \frac{\partial m}{\partial t} \quad (16)$$

but, from 12,

$$\bar{\rho} \frac{\partial^2 \bar{u}'}{\partial x \partial t} = -\frac{\partial^2 \bar{p}'}{\partial x^2} + \frac{\partial f}{\partial x}$$

substitute in (16)

$$\frac{1}{\bar{c}_p \bar{T}} \left[\frac{1}{\gamma - 1} \frac{\partial^2 \bar{p}'}{\partial t^2} - \frac{\partial q}{\partial t} + \frac{\bar{p}}{\gamma - 1} \frac{\partial^2 (\bar{M}'/\bar{M})}{\partial t^2} \right] - \frac{\partial^2 \bar{p}'}{\partial x^2} + \frac{\partial f}{\partial x} = \frac{\partial m}{\partial t} \quad (17)$$

Now $(\gamma - 1) \bar{c}_p \bar{T} = \gamma \bar{R}_g \bar{T} = \bar{c}^2$

(\bar{c} = speed of sound)

(18)

$$\frac{\partial^2 \bar{p}'}{\partial t^2} - \bar{c}^2 \frac{\partial^2 \bar{p}'}{\partial x^2} = \frac{\partial}{\partial t} \left[\bar{c}^2 m + (\gamma - 1) q - \bar{p} \frac{\partial (\bar{M}'/\bar{M})}{\partial t} \right] - \bar{c}^2 \frac{\partial f}{\partial x} \quad (19)$$

$$(\gamma - 1) \bar{C}_p \bar{T} \times \frac{\partial(15)}{\partial x} \rightarrow \bar{c}^2 \bar{\rho} \frac{\partial^2 u'}{\partial x^2} + \frac{\partial^2 p'}{\partial x \partial t} = (\gamma - 1) \frac{\partial q}{\partial x} + \bar{c}^2 \frac{\partial m}{\partial x} - \bar{p} \frac{\partial^2 (\mu' / \bar{\mu})}{\partial t \partial x} \quad (20)$$

$$\frac{\partial(9)}{\partial t} \rightarrow \bar{\rho} \frac{\partial^2 u'}{\partial t^2} + \frac{\partial^2 p'}{\partial x \partial t} = \frac{\partial f}{\partial t} \quad (21)$$

Subtract, divide by $\bar{\rho}$:

$$\boxed{\frac{\partial^2 u'}{\partial t^2} - \bar{c}^2 \frac{\partial^2 u'}{\partial x^2} = \frac{1}{\bar{\rho}} \frac{\partial f}{\partial t} - \frac{1}{\bar{\rho}} \frac{\partial}{\partial x} \left[\bar{c}^2 m + (\gamma - 1) q - \bar{p} \frac{\partial (M' / \bar{M})}{\partial t} \right]} \quad (22)$$

Note the combination $\bar{c}^2 m + (\gamma - 1) q - \bar{p} \frac{\partial (M' / \bar{M})}{\partial t}$

Adding heat, adding mass, or having a decrease rate of molecular mass, all are (up to factors) equivalent acoustic disturbances.

To close the problem, one needs to relate the perturbations (m , q , f , $\frac{\partial \mu'}{\partial t}$) to the state variables (p' , ρ' , u' , T'), by looking at the particular mechanisms (vaporization, combustion, etc), and how they depend on pressure, velocity, and so on.

General Conditions for Instability

Looking at Eq. (19), we see that the effects of gas mass generation m , heat generation q and molecular mass change $-\frac{\partial \mu' / \bar{\mu}}{\partial t}$ are similar. All of them have the effect of increasing the local volume, and we suspect therefore that when these quantities (acting together) peak when the pressure also peaks, we will have unstable condition.

To examine this, define the quantity

$$Q = \bar{c}^2 m + (\gamma - 1) q - \bar{p} \frac{\partial (M' / \bar{M})}{\partial t} \quad (23)$$

and ignore for now the local disturbing forces f . Then

$$\frac{\partial^2 p'}{\partial t^2} - \bar{c}^2 \frac{\partial^2 p'}{\partial x^2} = \frac{\partial Q}{\partial t} \quad (24)$$

For a sinusoidal wave of the type

$$p'(t) = R_e \left[\hat{p} e^{i(\omega t - kx)} \right] \quad (25)$$

with ω complex and k real, we then have

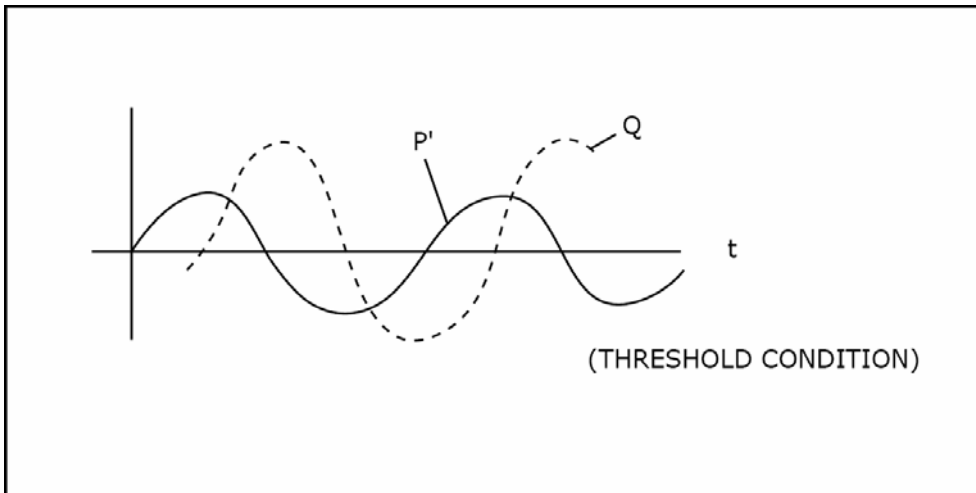
$$-\omega^2 \hat{p} + k^2 \hat{c}^{-2} \hat{p} = i\omega \hat{Q} \quad (26)$$

Define
$$v \equiv \frac{\omega}{kc}; \quad h = \frac{1}{2kc} \frac{i\hat{Q}}{\hat{p}} \quad (27)$$

and re-write (26) as
$$v^2 + 2hv - 1 = 0 \quad (28)$$

which has the complex solution
$$v = -h \pm \sqrt{1 + h^2} \quad (29)$$

We now ask what form h should have for stability. First, we note that at the stability threshold, v is real, and so $h = (1 - v^2) / 2v$ must also be real. From (27), this means that $i\hat{Q}$ must be in phase (or counter-phase) with \hat{p} , namely, “volume addition rate” must be 90° ahead of or behind pressure oscillations:



More generally, re-write (28) as $v + 2h - \frac{1}{v} = 0$, and put explicitly $h = h_r + ih_i$,

$$v = v_r + iv_i:$$

$$v_R + i v_I + 2 h_R + 2 i h_I - \frac{v_R - i v_I}{v_R^2 + i v_I^2} = 0 \quad (30)$$

Separate real and imaginary parts:

$$\left. \begin{aligned} v_R + 2h_R - \frac{v_R}{v_R^2 + v_I^2} &= 0 \\ v_I + 2h_I + \frac{v_I}{v_R^2 + v_I^2} &= 0 \end{aligned} \right\} \quad (31)$$

$$\text{From (31b), } h_I = -\frac{1}{2} v_I \left[1 + \frac{1}{v_R^2 + i v_I^2} \right] \quad (32)$$

This shows that whenever $h_I > 0$, $v_I < 0$. Since $p' \sim e^{i\omega t} = e^{-\omega_I t} e^{i\omega_R t}$, $v_I < 0$ implies instability. Also, from (27b), $h_I > 0$ implies $\left(\frac{\hat{Q}}{\hat{p}} \right)_R > 0$, which means that the "volume addition rate" $Q(t)$ must have a positive projection on pressure $p'(t)$, namely, a part in-phase with it. This is a confirmation of the physical intuition that releasing "volume" when pressure is high must be de-stabilizing. We repeat that this may mean heat addition, gas addition (vaporization) or molecular mass reduction rate (decomposition of complex molecules).

Let us now consider briefly the effect of body forces f . Returning to (19) and defining the complex quantity.

$$\rho = \frac{i \hat{f}}{k \hat{p}} \quad (33)$$

we can see that (28) is expanded to the form

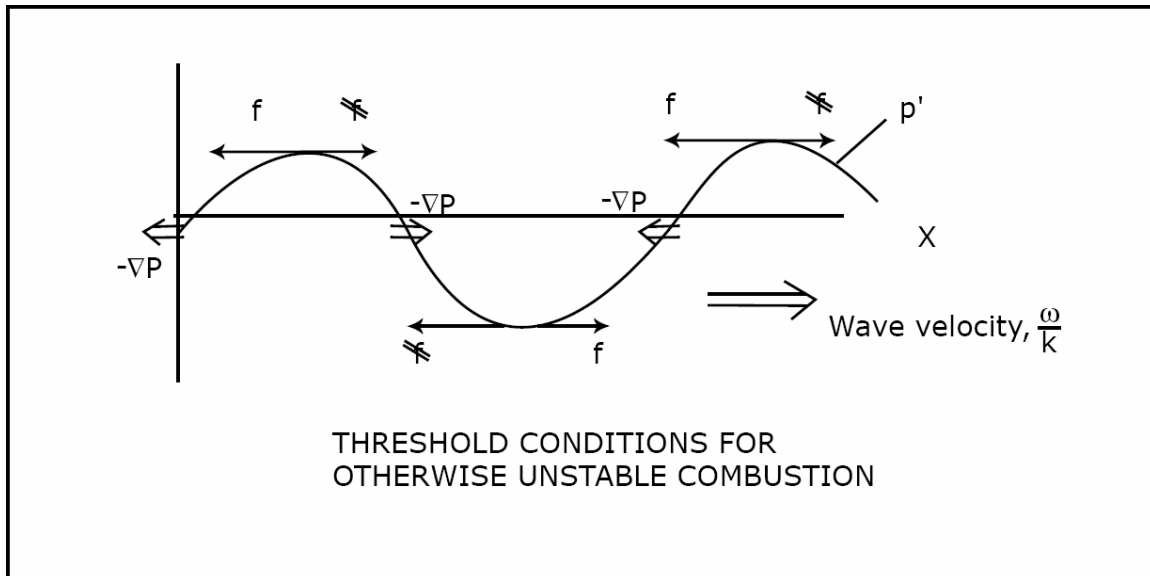
$$v^2 + 2h v (1 - \rho) = 0 \quad (34)$$

For neutral conditions (stability threshold), we must have real v ($v_I = 0$), so, taking the imaginary part of (34),

$$2v h_I + \rho_I = 0 \quad (35)$$

In the absence of forces, we found that $h_I > 0$ would lead to instability. We see now that if $\rho_I = -2v h_I$, which is negative, then the process stabilizes at least to the point of neutral stability. From (33), the conclusion is that $\left(\frac{\hat{f}}{\hat{p}} \right)_R < 0$ is stabilizing, i.e., the body forces should be in the backwards direction (against H velocity) when pressure is high, and vice-versa.

Looking at one instant of time vs. distance:



So, the body forces are in quadrature with the pressure gradient force ($-\nabla P$), and are taking energy away from the wave motion.

The "Sensitive time lag" theory (Harrje and Reardon, p.1)

Basic scenario:

- Drops injected at $t - \tau_r$ complete evaporation and combustion at
- However, from $t - \tau_r$ to $t - \tau$, no complete evaporation occurs, only "precursor processes". τ = "sensitive lag."
- The rate of evaporation + combustion during τ is sensitive to pressure and/or velocity. For p , $\frac{\partial \ln(\text{rates})}{\partial \ln P} \equiv n$ (1)
(n = "sensitivity index").
- The duration τ of actual evap. + comb. changes in time, in response to these rate changes. However, the total mass burnt is that of the drop, and it is assumed their mass (and their number) are independent of P , v in the chamber.

Say, R is the relevant rate. Under "quiet" or "mean" conditions, $R = \bar{R}$. When $P \neq \bar{P}$,

$$R \approx \bar{R} \left(1 + n \frac{p - \bar{p}}{\bar{p}} \right) \quad (2)$$

Express that the total mass burnt in $(t - \tau, t)$ is always the same, equal to that burnt under mean condition

$$\int_{t-\tau}^t \bar{R} \left(1 + n \frac{p - \bar{p}}{\bar{p}} \right) dt_1 = \int_{t-\bar{\tau}}^t \bar{R} dt_1 \quad (3)$$

$$\int_{t-\tau}^{t-\bar{\tau}} \bar{R} dt_1 + \bar{R} n \int_{t-\bar{\tau}}^t \frac{p - \bar{p}}{\bar{p}} dt_1 = 0$$

here replacing τ by $\bar{\tau}$ is ok.
(2nd order error)

$$\tau - \bar{\tau} = -n \int_{t-\bar{\tau}}^t \frac{p - \bar{p}}{\bar{p}} dt_1 \quad (4)$$

Let now, specifically, m be the rate of gas generation from liquid (local, per unit volume). The liquid injection rate is constant, equal to \bar{m} . The gas generated in $(t, t+dt)$ is $m dt$. This gas originates from liquid that reached its "maturity" for vaporization between $t - \tau$ and $(t - \tau) + d(t - \tau)$, and since liquid arrives at \bar{m} ,

$$m dt = \bar{m} d(t - \tau)$$

$$\frac{m - \bar{m}}{\bar{m}} = - \frac{d\tau}{dt} \quad (5)$$

From (4)
$$\frac{d\tau}{dt} = -n \frac{P(t) - P(t - \tau)}{\bar{p}}$$

and so
$$\boxed{\frac{m - \bar{m}}{\bar{m}} = n \frac{P(t) - P(t - \tau)}{\bar{p}}} \quad (6)$$

or, in terms of perturbations,
$$\boxed{\frac{m'}{\bar{m}} = n \frac{P'(t) - P'(t - \tau)}{\bar{p}}} \quad (6')$$

NOTE: Eq. (3) is wrong in Harrje and Reardon.

Control of Instabilities

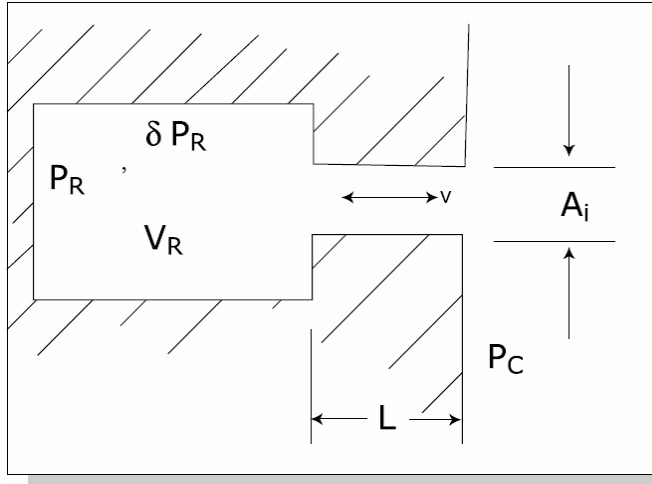
Despite all efforts at avoidance through design, the need remains for devices that will help damp the many potential modes of instability in any given rocket combustor. A new technology for active control is now evolving [31], in which feedback controlled acoustic generators are used to cancel unstable waves. Since the growth can be detected at small amplitude, it may not be necessary to inject very large acoustic powers for this purpose. Nevertheless, the mainstay of current practice is based on passive damping methods. A good description of these methods, with design guidelines, is given in Ref. 32.

The most important high frequency stabilization devices are injector head baffles and acoustic absorbers. Baffles are radial or circumferential barriers attached to the injector head and extending 0.1-0.2 diameters in the axial direction. An example of a baffled injector is that of the SSME (Fig. 3, from Ref. 2). The exact mechanism by which baffles enhance stability is not well understood, which has led to some divergence in design. It appears that the effect is related to the sensitivity of the droplet velocity cross-over point, which occurs quite close to the injector face, and it may involve disruption of the tangential gas motion associated with tangential modes, or shifting of the local acoustic frequencies to values above the characteristic drop vaporization frequencies.

Acoustic absorbers are cavities on the chamber walls with relatively narrow connecting channels to the chamber, so as to dissipate power during pressure oscillations in their vicinity. Their action is much better understood than that of baffles, and designers can proceed with some confidence, using methods described, for example in Ref. 32. Absorbers are often located on the cylindrical walls, near the injector, or as "corner slots" between injector and cylinder. They can also take the form of a continuous double wall with an array of holes periodically arranged to connect to the chamber. The absorption coefficient of a well-designed absorber can be high over a relatively wide frequency band, so as to contribute damping to the most prevalent modes. Sometimes several different absorbers are used, each tuned to a different frequency. Fig. 4 (Ref. 32) shows a baffled injector with corner absorbers, and Fig. 5 (Ref. 32) shows an extended acoustic liner.

A simplified analysis of an acoustic absorber is described next.

Acoustic Absorbers: Resonators



The schematic shows a device which is a variation on the Helmholtz Resonator concept.

Consider first the half-cycle during which flow is leaving the resonator ($\dot{m} > 0$). The pressure inside the resonator is P_R , while at the entrance to the narrow inlet duct, it is

$P'_R = P_R - \frac{1}{2} \rho v^2$, due to the (subsonic) acceleration towards the inlet. The density changes $\delta \rho$ can be equated to $\delta \rho / c^2$ ($c =$ speed of sound in the resonator).

The mass balance is then

$$\frac{V_R}{c^2} \frac{dP_R}{dt} = -\dot{m} \quad (1)$$

and the momentum balance in the duct is

$$\frac{d}{dt}(\rho A_i L v) = A_i (P'_R - P_C)$$

or, using $\dot{m} = \rho A_i v$,

$$\frac{d\dot{m}}{dt} = \frac{A_i}{L} \left(P_R - P_C - \frac{\dot{m}^2}{2\rho A_i^2} \right) \quad (2)$$

Consider next the other half-cycle, when the cavity is filling ($\dot{m} < 0$). The pressure at the chamber-side of the duct, which is now the flow inlet is

$P'_C = P_C - \frac{1}{2} \rho (-v^2)$, whereas that at the exit of the duct is now just P_R . Eq. (1) still holds, whereas the momentum balance is now

$$\frac{d\dot{m}}{dt} = \frac{A_i}{L} \left(P_R - P_C + \frac{\dot{m}^2}{2\rho A_i^2} \right) \quad (3)$$

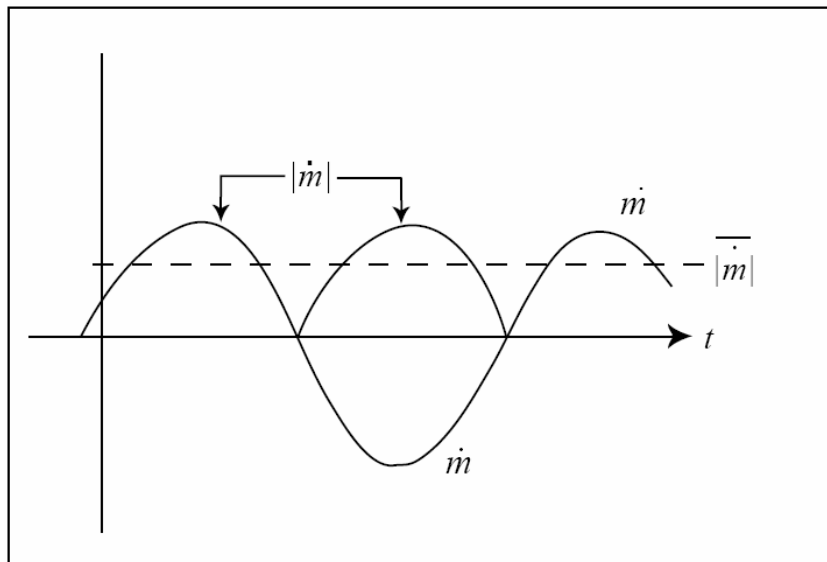
We now differentiate (2) and (3), and unify the two half-cycle momentum equations as

$$\frac{d^2 \dot{m}}{dt^2} = \frac{A_i}{L} \left(\frac{dP_R}{dt} - \frac{|\dot{m}|}{\rho A_i^2} \frac{d\dot{m}}{dt} - \frac{dP_c}{dt} \right)$$

Substituting Eq. (1) here,

$$\frac{d^2 \dot{m}}{dt^2} + \frac{|\dot{m}|}{\rho L A_i} \frac{d\dot{m}}{dt} + c^2 \frac{A_i}{LV_R} \dot{m} = -\frac{A_i}{L} \frac{dP_c}{dt} \quad (4)$$

This equation is non-linear in \dot{m} , but we can obtain reasonable results for steady state operation if we replace $|\dot{m}|$ by its time average over one cycle. The analysis reduces them to that of a forced linear oscillator, except that $|\dot{m}|$ needs to be calculated self-consistently rather than being a prescribed quantity.



Assume solutions of the form

$$\dot{m} = R_e \left[\hat{m} e^{i\omega t} \right], \quad \delta P_R = R_e \left[\hat{\delta P}_R e^{i\omega t} \right], \text{ etc.} \quad (5)$$

Eq. (4) becomes

$$\left(-\omega^2 + \frac{\overline{|\dot{m}|}}{\rho L A_i} i\omega + c^2 \frac{A_i}{L V_R} \right) \hat{m} = -i\omega \frac{A_i}{L} \hat{\delta p}_c \quad (6)$$

while Eq. (1) gives

$$i\omega \frac{V_R}{c^2} \hat{\delta P}_R = -\hat{m} \quad (7)$$

and solving (6) and (7) together,

$$\frac{\hat{\delta P}_R}{\hat{\delta p}_c} = \frac{\frac{c^2 A_i}{L V_R}}{\frac{c^2 A_i}{L V_R} + \frac{\overline{|\dot{m}|}}{\rho L A_i} i\omega - \omega^2} \quad (8)$$

From this, the natural frequency of the oscillations is seen to be $\omega_n = c \sqrt{\frac{A_i}{L V_R}}$ (9)

and the damaging factor ζ is given by

$$2\zeta\omega_n = \frac{\overline{|\dot{m}|}}{\rho L A_i}, \quad \text{or} \quad \zeta = \frac{\overline{|\dot{m}|}}{2\rho L A_i c} \sqrt{\frac{L V_R}{A_i}} \quad (10)$$

For the "rectified sine wave" $\overline{|\dot{m}|}$ (t), we can see that $\overline{|\dot{m}|} = \frac{2}{\pi} \hat{m}$, and from (7) and (8),

$$\overline{|\dot{m}|} = \frac{2}{\pi} \omega \frac{V_R}{c^2} \left| \hat{\delta P}_R \right| = \frac{2}{\pi} \omega \frac{V_R}{c^2} \frac{\frac{c^2 A_i}{L V_R}}{\left| \frac{c^2 A_i}{L V_R} + \frac{\overline{|\dot{m}|}}{\rho L A_i} i\omega - \omega^2 \right|} \left| \hat{\delta p}_c \right| \quad (11)$$

Using $\left| \frac{c^2 A_i}{L V_R} - \omega^2 + \frac{\dot{m}}{\rho L A_i} i \omega \right| = \sqrt{\left(\frac{c^2 A_i}{L V_R} - \omega^2 \right)^2 + \left(\frac{\dot{m}}{\rho L A_i} \right)^2} \omega^2$, this yields a bi-quadratic

equation for \dot{m} in terms of the amplitude δP_c of the pressure fluctuations in the chamber. The algebra is simpler in non-dimensional terms. Define

$$\left\{ \begin{array}{l} \nu \equiv \frac{\omega}{\omega_n} = \frac{\omega}{c} \sqrt{\frac{L V_R}{A_i}} \end{array} \right. \quad (12)$$

$$\left\{ \begin{array}{l} \rho \equiv \frac{2}{\pi} \frac{V_R}{L A_i} \frac{|\delta P_c|}{\frac{1}{2} \rho c^2} \end{array} \right. \quad (13)$$

We then obtain $\left| \dot{m} \right|^2 = \frac{1}{2} \left(\frac{\rho c^2 A_i^2}{\omega V_R} \right)^2 \left[-(1-\nu^2)^2 + \sqrt{(1-\nu^2)^4 + \rho^2 \nu^4} \right]$, and substituting in (10), the damping ratio is

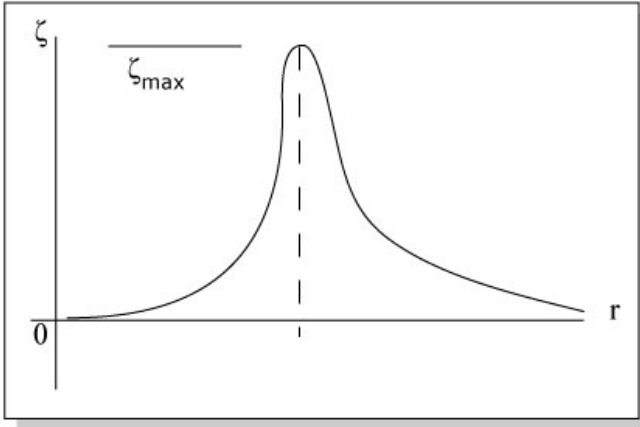
$$\zeta^2 = \frac{\rho^2 \nu^2 / 2}{(1-\nu^2)^2 + \sqrt{(1-\nu^2)^4 + \rho^2 \nu^4}} \quad (14)$$

Several points can now be made:

- For any frequency, the damping increases with pressure fluctuation intensity. This is a favorable circumstance because we need the damping most when combustion is rough. Mathematically, this is a consequence of the non-linearity of the equation. Physically, energy is dissipated both during aspiration and during expulsion of gas from the cavity, (by the mixing out of the jet kinetic energy), and it is clear that more energy is dissipated when the driving pressure differences are stronger.
- Although the algebra is still tedious, differentiation of (14) shows that ζ is maximum at $\nu = 1$, i.e., when the cavity is tuned in resonance with the pressure fluctuations (by selecting parameters so that $\omega_n = \omega$). Putting $\nu = 1$ in (14) gives

$$\zeta_{MAX} = \sqrt{\rho / 2} = \sqrt{\frac{V_R}{\pi L A_i}} \sqrt{\frac{|\delta P_c|}{\frac{1}{2} \rho c^2}} \quad (15)$$

which again shows ζ increasing with fluctuation intensity.



(c) Since we should design for resonance for the given ω , the dimensions should satisfy $\frac{A_i}{LV_R} = \frac{\omega^2}{c^2}$. Eq. (15) can then be put in the two equivalent forms

$$\zeta_{MAX} = \frac{1}{\omega L} \sqrt{\frac{2}{\pi} \frac{\hat{\delta P}_c}{\rho}} = \omega \frac{V_R}{A_i} \sqrt{\frac{2}{\pi} \frac{\hat{\delta P}_c}{\rho}} \quad (16)$$

This indicates we should use short inlets, large cavity volumes and small inlet areas (subject to $\frac{A_i}{LV_R} = \frac{\omega^2}{c^2}$).

As an indication of what is possible, consider 1% fluctuations on a pressure P_c such that $\frac{P_c}{\rho} = R_g T_c$ is $\frac{P_c}{\rho} = \frac{8.3}{0.02} \times 3000 = 1.25 \times 10^6 \text{ m}^2 / \text{s}^2$. The acoustic frequency to be damped is at $f = 2000 \text{ Hz}$, or $\omega = 2\pi f = 12,500 \text{ m/s}$. Then from the first of Eqs. (16), we can obtain critical damping ($\zeta_{MAX} = 1$) by choosing an inlet length

$$L = \frac{1}{\omega \zeta_{MAX}} \sqrt{\frac{2}{\pi} \frac{\hat{\delta P}_c}{\rho}} = \frac{1}{12,500} \sqrt{\frac{2}{\pi} (1.25 \times 10^4)} = 7.2 \times 10^{-3} \text{ m} = \underline{7.2 \text{ mm}}$$

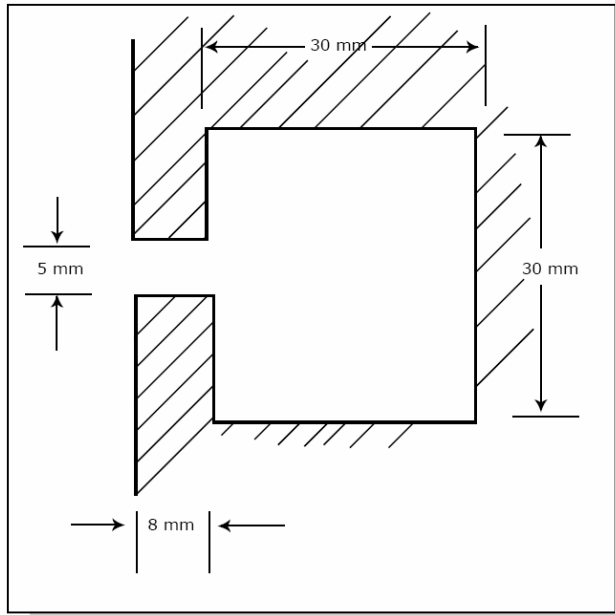
which appears reasonable. To ensure resonance, then, we need to select.

$$\frac{V_R}{A_i} = \frac{c^2}{\omega^2 L} = \frac{\gamma R_c T_c}{\omega^2 L} \approx \frac{1.2 \times 1.25 \times 10^6}{(12,500)^2 \times 7.2 \times 10^{-3}} = 1.34 \text{ m}$$

A possible choice of geometry is then to take an inlet diameter of, say, 5mm, and a cavity volume

$$V_R = 1.34 \frac{\pi}{4} 0.005^2 = 2.63 \times 10^{-5} \text{ m}^3 = 26.3 \text{ cm}^3$$

If this is shaped as a cubic cavity, its side is about 3 cm. These dimensions are sketched (roughly to scale) below.



As a final note, remember that the “lumped parameter” idealization used in the theory may not be very precise. Only semi-quantitative accuracy is to be expected, but the trends should be correct and the analysis can be used for preliminary design, to be refined through numerical simulation or physical testing.

How many acoustic dampers:

$$\delta \xi_{SR}^E = \frac{1}{2} \left| \delta \dot{m} \right| v^2 + \rho \delta P_R V_R =$$

$$\frac{d(\delta \xi_{SR}^E)}{dt} = \frac{1}{2} \left| \delta \dot{m} \right| v \delta v + \frac{d\delta P_R}{dt} V_R \quad v = \frac{\dot{m}}{\rho A_i} \quad \delta v = \frac{\delta \dot{m}}{\rho A_i}$$

With no dissipation

$$\left. \begin{aligned} \frac{d\dot{m}}{dt} &= \frac{A_i}{L} (P_R - P_C) \\ \dot{m} &= -\frac{V_R}{c^2} \frac{dP_R}{dt} \end{aligned} \right\} \begin{cases} \frac{d\delta \dot{m}}{dt} = \frac{A_i}{L} \delta P_R & \frac{L}{A_i} \delta \dot{m} \\ \frac{d\delta P_R}{dt} = -\frac{c^2}{V_R} \delta \dot{m} & \frac{V_R}{c^2} \delta P_R \end{cases}$$

$$\frac{d}{dt} \left(\frac{L}{A_i} \delta \dot{m} + V_R \frac{\delta P_R}{c^2} \right) = 0 \quad \times c^2 \quad \frac{d}{dt} \left(\frac{L}{A_i} c^2 (\delta \dot{m})^2 + V_R (\delta P_R)^2 \right) = 0$$

$$\zeta_R = \frac{\frac{L}{A_i} c^2 (\delta \dot{m})^2 + V_R (\delta P_R)^2}{2 \rho c^2} = \frac{L}{2 \rho A_i} (\delta \dot{m})^2 + \frac{V_R}{2 \rho c^2} (\delta P_R)^2$$

With dissipation

$$\left. \begin{aligned} \frac{d \delta \dot{m}}{dt} &= \frac{A_i}{L} \left(\delta P_R - \frac{|\dot{m}| \delta \dot{m}}{\rho A_i^2} \right) \\ \frac{d(\delta P_R)}{dt} &= -\frac{c^2}{V_R} \delta \dot{m} \end{aligned} \right\} \begin{array}{l} \frac{c^2 L}{A_i} \delta \dot{m} \\ V_R \delta P_R \end{array}$$

$$\frac{d}{dt} \left[\frac{L}{A_i} c^2 (\delta \dot{m})^2 + V_R (\delta P_R)^2 \right] = \frac{|\dot{m}|}{2 \rho^2 A_i^2} (\delta \dot{m})^2 \quad (\text{energy dissipation rate}) \quad \zeta_R$$

Average $\overline{\dot{\varepsilon}_R} = \frac{|\dot{m}|^3}{2 \rho^2 A_i^2} \quad \left| \dot{m} \right| = \frac{2}{\pi} \left| \hat{m} \right|$

At resonance, $\hat{m} = -\frac{A_i}{L} \hat{\delta P}_c \quad \frac{\rho L A_i}{|\dot{m}|} = -\frac{\rho A_i^2}{|\dot{m}|} \hat{\delta P}_c$

$$\left| \dot{m} \right| = \frac{2}{\pi} \frac{\rho A_i^2}{|\dot{m}|} \left| \hat{\delta P}_c \right| \quad \left| \dot{m} \right| = \sqrt{\frac{2}{\pi} \rho A_i^2 \left| \hat{\delta P}_c \right|}$$

$$\overline{\dot{\varepsilon}_R} = \frac{1}{2 \rho^2 A_i^2} \left(\frac{2}{\pi} \rho A_i^2 \left| \hat{\delta P}_c \right| \right)^{3/2} = \frac{1}{2} \left(\frac{2}{\pi} \right)^{3/2} \frac{A_i}{\sqrt{\rho}} \left| \hat{\delta P}_c \right|^{3/2}$$

Average chamber acoustic energy $\bar{\xi}_c = V_c \frac{|\hat{\delta P}_c|^2}{\rho c^2}$

$$(\Delta\omega)_c = N \frac{1}{2} \frac{\dot{\xi}_R}{\xi_c} = \frac{1}{2} \frac{N}{2} \left(\frac{2}{\pi}\right)^{3/2} \frac{A_i}{\sqrt{\rho}} \frac{\rho c^2}{V_c \sqrt{\hat{\delta P}_c}} = \frac{\sqrt{2}}{2\pi^{3/2}} \frac{NA_i}{V_c} c^2 \sqrt{\frac{\rho}{\hat{\delta P}_c}}$$

contribution of ω_i of chamber, due to N resonators

Also, $(\omega_n)_c = (\omega_n)_R = c \sqrt{\frac{A_i}{LV_R}}$

$$\Delta\zeta_c = \frac{(\Delta\omega)_c}{\omega_n} = \frac{1}{\sqrt{2\pi^3}} \frac{NA_i}{V_c} c^2 \sqrt{\frac{\rho}{\hat{\delta P}_c}} \frac{1}{c} \sqrt{\frac{LV_R}{A_i}} = \frac{1}{\sqrt{2\pi^3}} \frac{N}{V_c} \sqrt{LV_R A_i} \sqrt{\frac{\rho c^2}{\hat{\delta P}_c}}$$

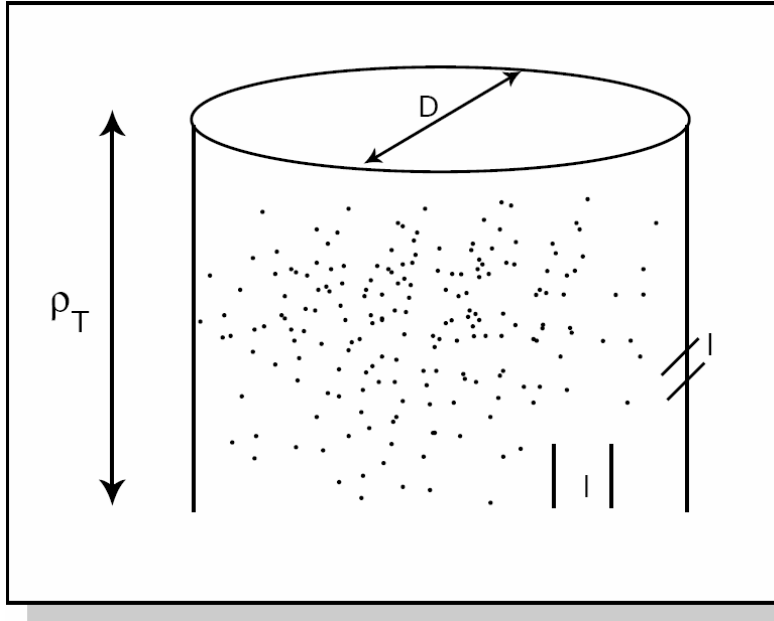
Example $\omega = 2\pi \times 2000\text{Hz}$ $\frac{\delta P_c}{\rho c^2} = \frac{1.25 \times 10^4}{1.2 \times 1.25 \times 10^6} = \frac{1}{120}$

$L = 7.2 \times 10^{-3} \text{ m}$ $V_R = 2.63 \times 10^{-5} \text{ m}^3$ $A_i = \frac{\pi}{4} 25 \times 10^{-6} \text{ m}^2$

and say $V_c = 0.1 \text{ m}^3$

$$\Delta\zeta_c = \frac{1}{\sqrt{2\pi^3}} \frac{N}{0.1} \sqrt{7.2 \times 10^{-3} \times 2.63 \times 10^{-5} \times 25 \frac{\pi}{4} \times 10^{-6}} \sqrt{120} = 2.7 \times 10^{-5} N$$

So, for $\Delta\zeta_c = 0.1$, need 3730 dampers.



Say $l = 4 \text{ cm}$
 $D = 40 \text{ cm}$

$$N = \frac{\pi D l \rho_T}{l^2} \quad l_T = \frac{N l^2}{\pi D} = \frac{3730 \times 16}{\pi \times 40} = 475 \text{ cm}$$

Not enough room

Can get $\sim \Delta \zeta = 0.02$ in $l_T = 1 \text{ m}$